

FIFTH AUSTRALASIAN CONFERENCE

on

HYDRAULICS AND FLUID MECHANICS

at

University of Canterbury, Christchurch, New Zealand

1974 December 9 to December 13

THE DEVELOPMENT OF A WAVE PACKET IN THE
BOUNDARY LAYER OF A FLAT PLATE

by

M. Gaster and I. Grant

S U M M A R Y

A short duration disturbance pulse was injected into the boundary layer of a flat plate at a point on the surface and hot-wire anemometer signals created by the passage of the resulting wave packet were recorded. Comparisons are made with a theoretical model of a wave packet which is generated by the summation of spatially growing eigenmodes of all frequencies and spanwise wavenumbers.

M. Gaster, National Physical Laboratory, Middlesex, U.K.

I. Grant, Physics Department, University of Edinburgh, U.K.

Introduction

Travelling-wave disturbances arise quite naturally during the initial stages of transition from a laminar to a turbulent boundary layer when the external turbulence level is sufficiently low. These waves, which are almost periodic, propagate downstream and amplify as they pass through any unstable regions of the flow. The initial development and growth is given by the linear theory of hydrodynamic stability. Experimental verification of this theory has been achieved mainly through the use of a wave maker, often a vibrating ribbon close to the surface, which generates two-dimensional periodic waves. Here the excitation of the unstable boundary layer takes the form of a short duration disturbance applied at a point on the surface. Measurements are reported of the resulting patch of unsteady flow as it moves downstream. Wave packets form through selective amplification and interference of the excited modes; they contain a spectrum of modes and are in some respects similar to the modulated disturbances generated by natural random excitation. In the initial phase of development of a packet, modes from which it is composed are uncoupled and can be treated adequately by linear theory. The disturbance can be evaluated in terms of an integral of isolated modes taken over all frequencies and spanwise wavenumbers. Previous solutions [see Brooke Benjamin (1961), Criminale and Kovasnay (1962), Gaster (1968) and Gaster and Davey (1968)] have used asymptotic methods to obtain approximations to the flow far downstream. These techniques, although useful in giving analytical expressions, are strictly not appropriate to the experimental situation where solutions at relatively small distances from the source are required. Here this difficulty is overcome by using a direct numerical summation to evaluate the integral.

Experiment

The experiment was carried out on the boundary layer generated by a 6ft. long elliptic nosed Perspex plate mounted in the 4ft. x 4ft. low-turbulence tunnel at Edinburgh University. An impulsive disturbance was injected into the flow at some upstream station and the resulting flow oscillations were monitored at various downstream locations. A small loudspeaker was attached to the back of the plate and excitation was provided through a hole of 20×10^{-3} in. dia. positioned on the centre line 12 in. from the leading edge. The disturbed flow was monitored by a hot-wire anemometer placed just outside the boundary layer at 1.1δ , where the velocity perturbation has a maximum, at various spanwise (z) and streamwise (x) locations. The pulse driving the speaker was set to a level low enough to avoid any obvious non-linear behaviour, which appeared as distortions of the wave packet records on an oscilloscope. The experiment was carried out at a free stream velocity of 38.3ft./sec.

Hot-wire signal records were obtained for spanwise locations in $\frac{1}{2}$ ins. steps covering the range $\pm 7\frac{1}{2}$ in. about the centre line at six streamwise stations from 18 in. to 48 in. in 6 in. steps. The signals were digitized and stored on a small on-line computer. Since the signal-to-noise ratio was rather poor it was necessary to generate repetitive phase-locked signals which were then averaged by the computer and written on to magnetic tape. Figure 1 compares a raw single-shot record with the average of 256 records. This process reduced the uncorrelated noise component by a factor of $\sqrt{256}$ and therefore increased the signal-to-noise by about 16. Further smoothing of the data was carried out by digital filtering, accomplished by reconstructing the signals from suitably weighted Fourier coefficients. This process, which used complex arithmetic routines, also generated the conjugate function which was of similar shape to the signal but with the oscillations 90° out of phase. These two functions, combined by taking the square root of the sum of the squares, formed the envelope. Figure 2 shows the filtered record of Figure 1 together with the envelope. All the records stored on magnetic tape were processed in this way to produce smoothed versions of the signal records and envelopes at each of the chosen locations. Sets of records covering the region $\pm 7\frac{1}{2}$ ins. about the centre line characterize the wave packet as it sweeps through each downstream position. An impression of the growth pattern and spread of the disturbed region as the packet progresses downstream can be obtained from the contours of the envelope amplitudes plotted on the $z \sim t$ plane on Figure 4. Details of the wave-like nature of the packet are revealed by the perspective projections of the signals displayed on Figure 6.

Theory

Before attempting to evaluate the solution to the complete problem of the flow created by an impulsive disturbance at a point, it is convenient to consider first the simpler case of the generation of two-dimensional waves by a wavemaker. A vibrating ribbon exciter of the type used by Schubauer and Skramstad (1948) undergoing simple harmonic oscillation can be expected to generate a whole spectrum of eigenmodes at the driving frequency. The higher modes decay rapidly and a few wavelengths downstream the motion is dominated by a single mode. In the subsequent downstream development of a disturbance these higher modes may safely be neglected. The eigenvalues, defining the wavelength and amplification, are found from those solutions of the equations of motion of the perturbation which are compatible with the usual boundary

conditions. In the case of a parallel flow the relevant equations separate and the eigenvalues are given by an ordinary differential equation - the Orr-Sommerfeld equation. Boundary layers grow quite slowly, like R_x^{-2} , and the approximation is generally made that the modes follow local eigenvalues appropriate to that location calculated from the Orr-Sommerfeld equation.

The development of such a wave is given by the integral

$$\sim e^{i \left[\int_{x_0}^x a(x) dx - \omega t \right]}$$

where ω is the real excitation frequency and $a(x)$ is the local streamwise wavenumber. To make some partial correction for the increase in boundary layer thickness with distance downstream a weak algebraic factor, x^{-4} , was included so that the local rate of growth of the integrated kinetic energy across the flow equated roughly with that given by the quasi-parallel flow treatment. The effect of weak mean flow deviations from the parallel can now be properly accounted for (see Bouthier 1972 and 1973 and Gaster 1974), and although the present factor of x^{-4} is probably not strictly correct it has nevertheless been retained here in an attempt to make some correction, at least, for flow divergence.

The disturbance generated by a pulsed point source may be found by summing all oblique spatially growing modes over all frequencies and spanwise wavenumbers.

$$\sim \int_0^\infty \int_0^\infty \lambda(b, \omega) x^{-4} e^{i \left[\int a(x) dx + bz - \omega t \right]} db d\omega,$$

$\lambda(b, \omega)$ is an algebraic function of b and ω which has been introduced to take account of the variation in response of the various modes. Since this function is expected to be relatively slow compared with the exponential term which dominates the behaviour downstream, treating it as a constant can be taken as a reasonable approximation. Eigenvalues, $a(x)$, were obtained for suitable values of both b and ω covering the most significant modes. The computation of eigenvalues was accomplished by a shooting technique using a Runge-Kutta integration routine. Spurious divergent solutions, which arise in such numerical processes from rounding errors, were eliminated by the filtering technique developed by Kaplan (1964). The neutral stability loop for two-dimensional waves was found to be virtually identical to that of Jordinson (1970). Oblique modes (non-zero values of b) were found from the Orr-Sommerfeld equation with complex values of the Reynolds number through Squire's (1933) transformation. In all, some 10,000 eigenvalues were computed and stored on magnetic tape. The streamwise integral of $a(x)$ was evaluated for each mode defined in terms of b and ω . This information enabled records of the simulated wave packet to be generated at the values of z and t used in the experiment, by evaluating the double integral for appropriate values of x by direct summation. The results of these computations, when suitably scaled, may be directly compared with experimental data. Figure 5, showing the envelope contours for the various downstream locations, may be compared with the experimental data of Figure 4. The numerical data from the theoretical model can be displayed as perspective projections (Figure 7) and these pictures, which relate to the wave-like character of the disturbed patch of fluid, can be compared with measurements on Figure 6.

Discussion

The experimental results describe the behaviour of a wave packet as it propagates downstream in a growing boundary layer. They show that the disturbance, initially covering a roughly elliptical region, gradually expands and becomes distorted into a kidney shape through the slightly lower propagation velocity of the outermost (large z) region. The measured amplitude contours spread out in an almost linear fashion in both z and t as the patch progresses downstream. In the early stages of development the peak amplitudes arose on the centre line, but at the 42in. station, where the signals increased rapidly, two peaks appeared symmetrically disposed about the centre. The perspective pictures of the disturbed region are perhaps the most informative outcome of the work. They show some of the detailed structure and how the smoothly curved wave crests become progressively distorted with distance travelled.

The theoretical model indicates a somewhat simpler pattern of behaviour. The envelope contours show very similar development to that observed over the first few stations. Later stages of the evolution of the simulated wave packet continue these trends and do not show the periodic spanwise structure observed in the experiment. The perspective projections are also quite similar to those of the experiment up to and including the 36in. station, but again the observed distortion of the wave fronts does not occur in the model pictures which continue to exhibit smooth wave patterns far downstream.

A more detailed comparison between theory and experiment is given on Figure 3 by the signals and envelopes from positions on the centre line of the packet for various distances from the source. The experimental data shows quite clearly how the initially smooth envelope, enclosing about two waves, spreads out to cover a region of five or so. The leading edge of the wave packet propagates downstream at a velocity of 0.44 of the free stream value, while the trailing edge ray settles down to a value of 0.36 after the transient has decayed away from the source. The envelopes show how a slight dimple close to the leading ray at the 36 in. position gradually develops into a deep valley at the 48in. location. The simulated records are more regular and do not have any indication of this distortion.

Concluding remarks

The observed rates of spread, the outline shapes of the wave packet and much of the detailed structure within the packet are predicted quite well by the linear model and some explanation must be found for the gradual deterioration of this correlation downstream. Since no mean flow survey had been carried out the spanwise uniformity was unknown. Any variations in boundary layer thickness across the span could well explain the wave crest warping and may also have been the cause of the development of the two amplitude maxima. However, the observed type of modulation, which is associated with the formation of the two amplitude peaks, suggested that non-linearity may be present. While setting up the experiment similar distorted signals were observed when the driving level to the speaker was high. Without further experimental work covering a range of excitation levels it is not possible to be certain whether this was the major cause of the differences between the model calculations and the observations, but it does seem to offer a likely explanation.

The experimental part of this work was carried out at Edinburgh University while one of the authors (M. Gaster) was a visitor to the Fluid Mechanics Unit of the Department of Natural Philosophy.

References

- Bouthier, M. 1972, *Journal de Mecanique*, 11, 599.
- Bouthier, M. 1973, *Journal de Mecanique*, 12, 75.
- Brooke Benjamin, T. 1961, *J. Fluid Mech.*, 10, 401.
- Criminale, W.O. and Kovasnay, L.S.G. 1962, *J. Fluid Mech.*, 14, 59.
- Gaster, M. 1968, *J. Fluid Mech.*, 32, 173.
- Gaster, M. 1974, To be published in *J. Fluid Mech.*
- Gaster, M. and Davey, A. *J. Fluid Mech.*, 32, 801.
- Jordinson, R. 1970, *J. Fluid Mech.*, 43, 801.
- Kaplan, R.E. 1964, M.I.T. Report ASRL-TR 116-1.
- Schubauer, G.B. and Skramstad, H.K. 1948, NACA Rep. 909.
- Squire, H.B. 1933, *Proc. Roy. Soc. A* 142, 621.

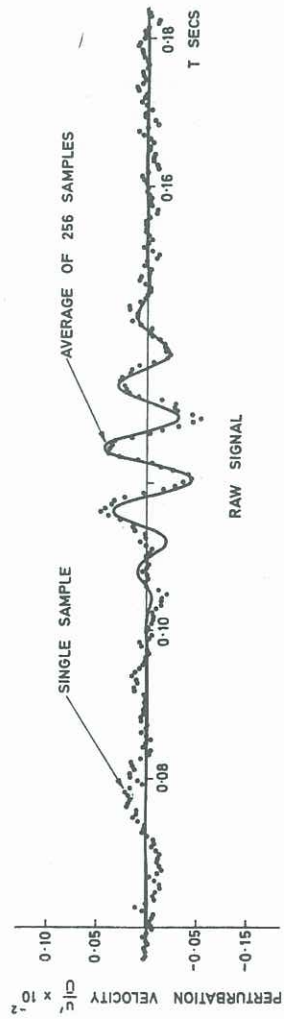


Figure 1

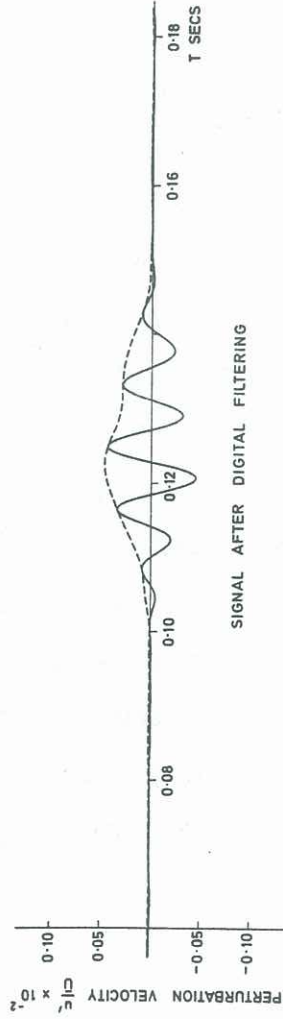
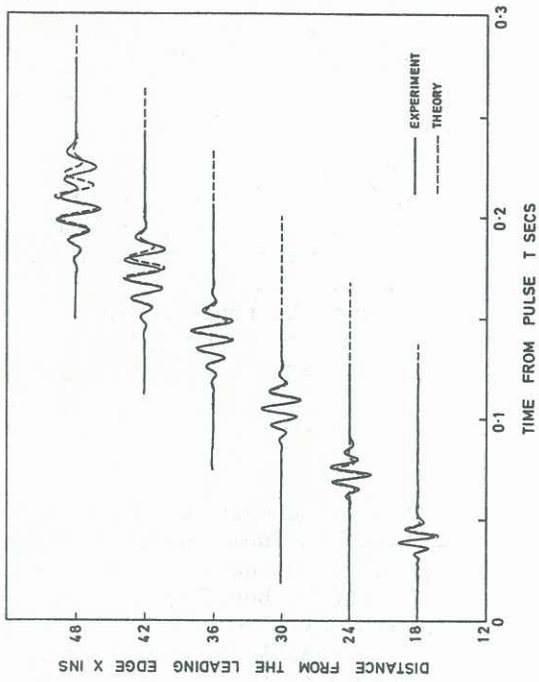
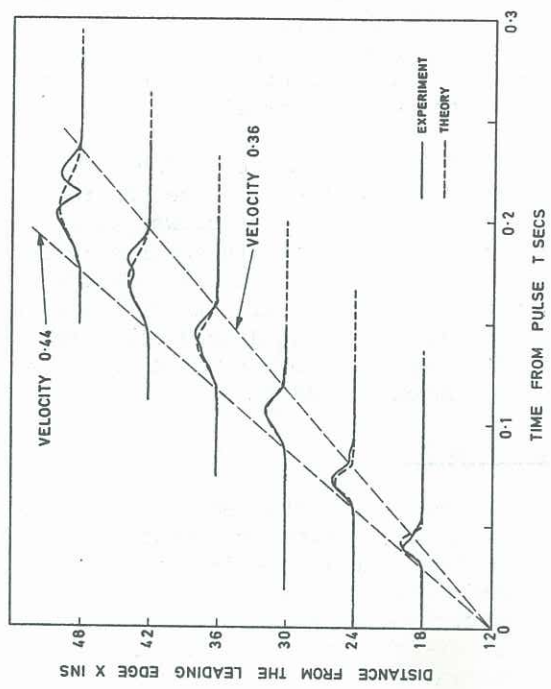


Figure 2

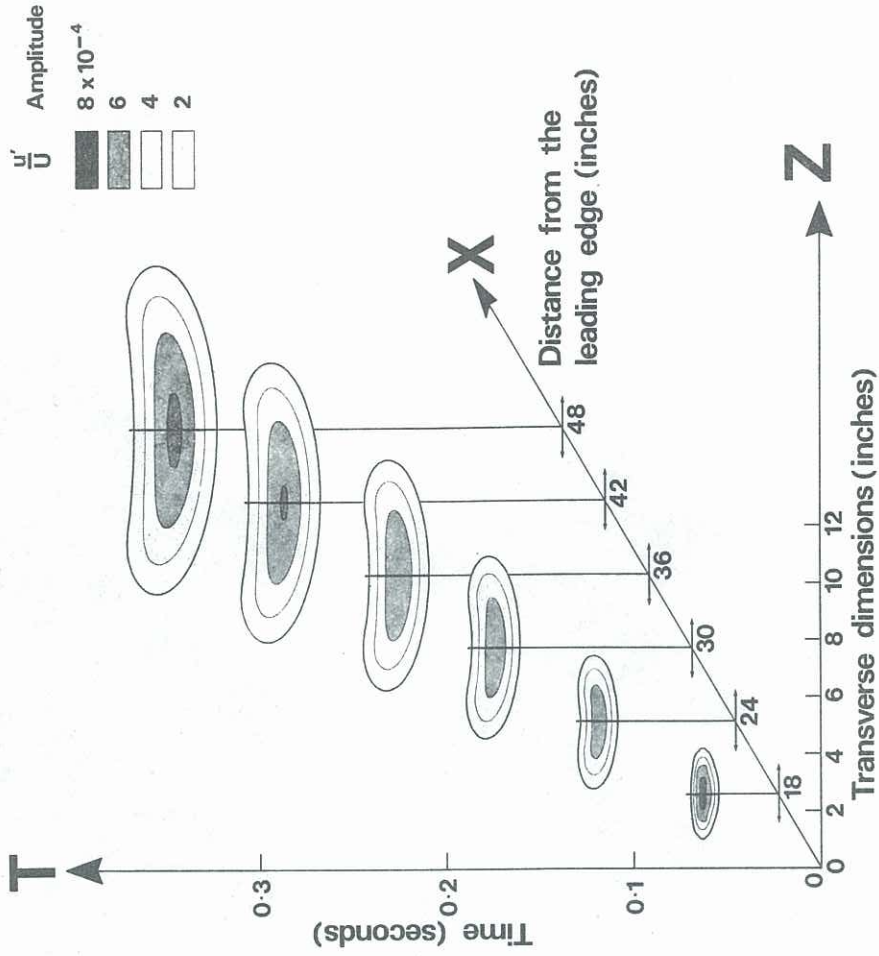


DEVELOPMENT OF THE WAVE PACKET ALONG THE CENTRE LINE



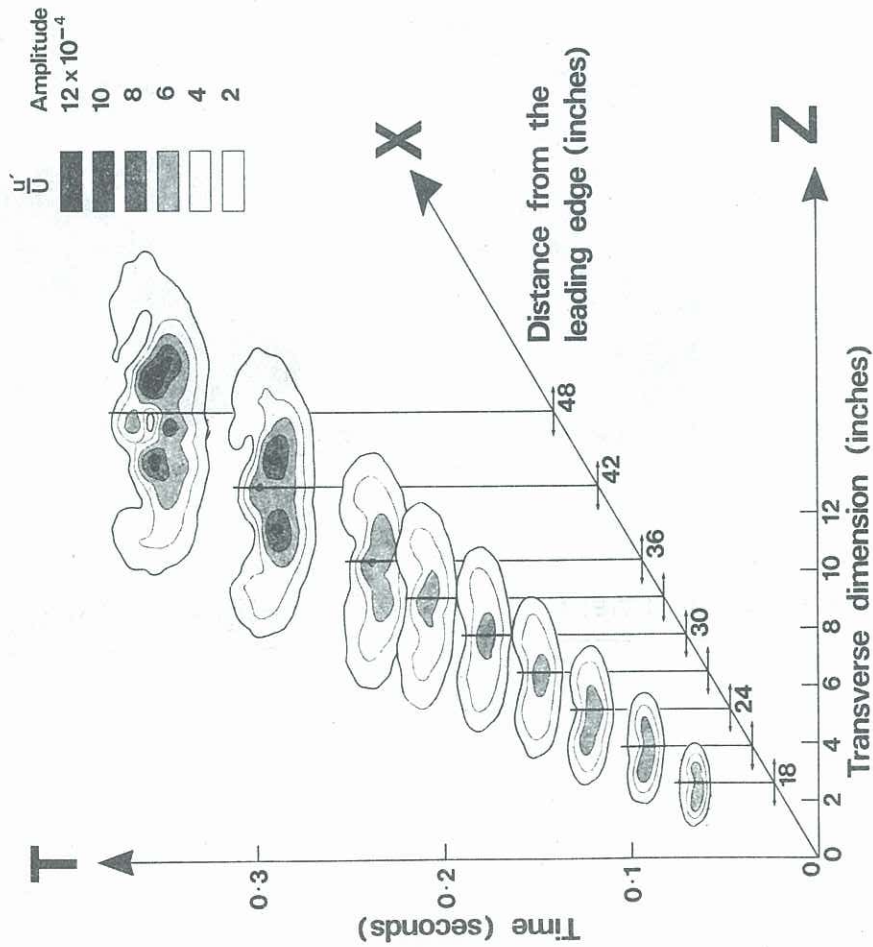
DEVELOPMENT OF THE WAVE ENVELOPE ALONG THE CENTRE LINE

Figure 3



Theoretical Amplitude Contours

Figure 5



Experimental Amplitude Contours

Figure 4

DEVELOPMENT OF THE WAVE PACKET
ALONG THE PLATE

X 48 INS.
 T_0 0.157 SECS.

X 42 INS.
 T_0 0.128 SECS.

X 36 INS.
 T_0 0.094 SECS.

X 30 INS.
 T_0 0.063 SECS.

X 24 INS.
 T_0 0.031 SECS.

X 18 INS.
 T_0 0 SECS.

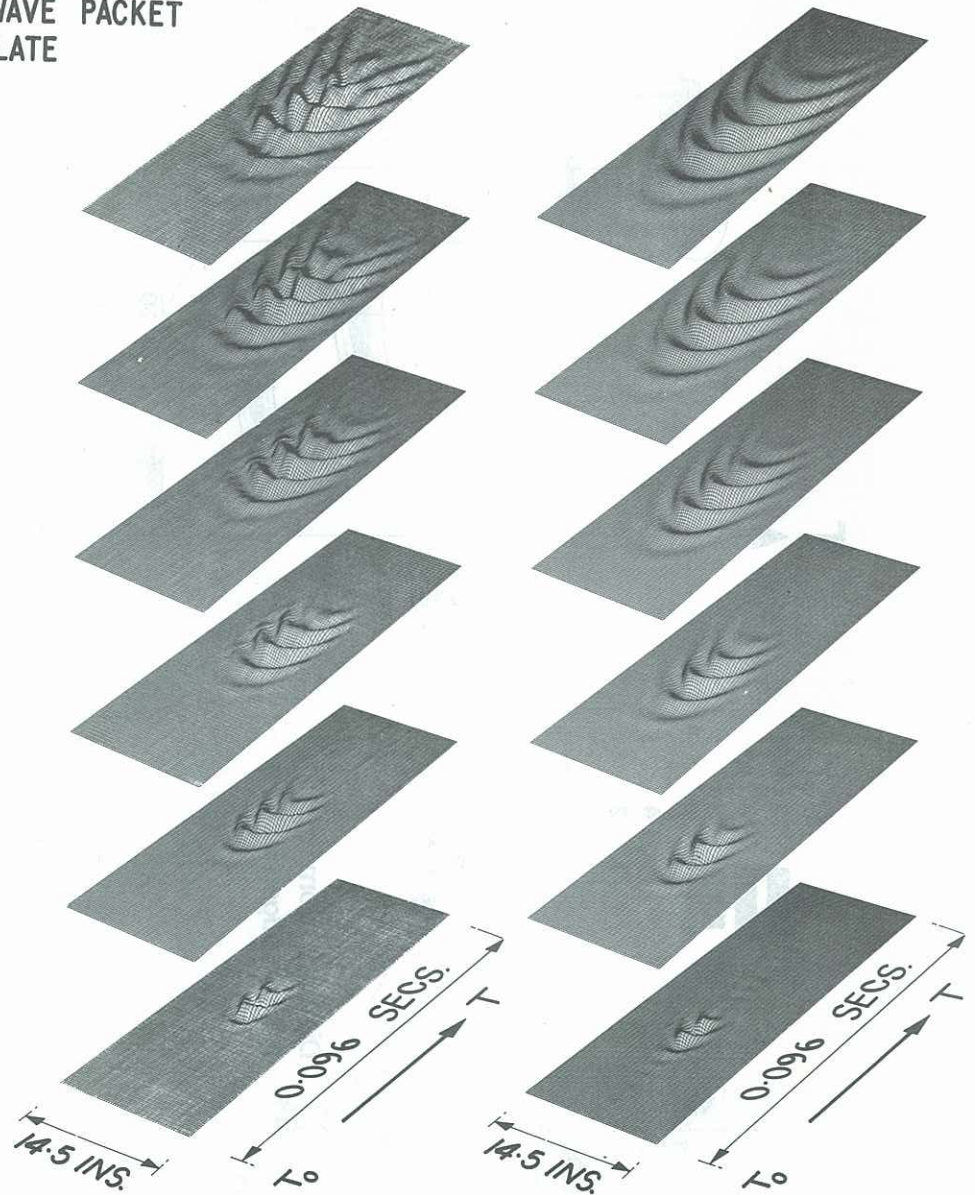


Figure 6 Experiment

Figure 7 Theory